



Available online at [www.sciencedirect.com](http://www.sciencedirect.com)

**ScienceDirect**

Journal of the Franklin Institute 359 (2022) 2445–2462

[www.elsevier.com/locate/jfranklin](http://www.elsevier.com/locate/jfranklin)



# Data-driven ILC algorithms using AFD in frequency domain for unknown linear discrete-time systems

Wen-Yuan Fu<sup>a,b</sup>, Xiao-Dong Li<sup>a,c,\*</sup>, Tao Qian<sup>d</sup>

<sup>a</sup>*School of Intelligent Systems Engineering, Sun Yat-sen University, Guangzhou 510006, China*

<sup>b</sup>*College of Information Science and Engineering, Huaqiao University, Xiamen 361002, China*

<sup>c</sup>*School of Information Science, Guangzhou Xinhua University, Dongguan 523133, China*

<sup>d</sup>*Macau Centre for Mathematical Sciences, Macau University of Science and Technology, Macau, China*

Received 23 April 2021; received in revised form 27 October 2021; accepted 8 February 2022

Available online 15 February 2022

---

## Abstract

In conventional PID-type iterative learning control (ILC) designs, to determine the learning control gains involved, relevant model knowledge on the controlled systems is often dependent. In this paper, two completely data-driven ILC laws, the extended PD-type ILC law and the extended P-type ILC law, are designed in frequency domain for linear discrete-time (LDT) single-input single-output (SISO) systems. The designs of the proposed ILC laws are based on the approximation/identification to unknown transfer function with a novel adaptive Fourier decomposition (AFD) technique. As a result, the strictly monotonic convergence of ILC tracking error is guaranteed in a deterministic way. A numerical example on a four-axis robot arm is performed to illustrate the effectiveness of the proposed data-driven ILC algorithms

© 2022 The Franklin Institute. Published by Elsevier Ltd. All rights reserved.

---

\* Corresponding author at: School of Intelligent Systems Engineering, Sun Yat-sen University, Guangzhou 510006, China.

*E-mail address:* [lixd@mail.sysu.edu.cn](mailto:lixd@mail.sysu.edu.cn) (X.-D. Li).

## 1. Introduction

Iterative learning control (ILC) is an effective control methodology for reducing tracking errors from trial-to-trial for dynamical systems that execute a given tracking task repeatedly over a finite time interval. During an ILC process, the control inputs are updated iteratively after each trial by using previous or current tracking errors such that the tracking performance of the controlled system is improved progressively. Recent three decades have witnessed considerable achievements in ILC theoretical development [1,5,7,14,15] with extensive applications in robot manipulators [2,32], batch processes [3], and 3-D crosswind flight [4], etc.

Hitherto, the existing ILC techniques can be roughly classified as PID-type and adaptive-type algorithms. The PID-type ILC algorithms were normally derived by the contraction mapping-based designs [8,10,29], 2-D analysis techniques [5,9,30], and norm-optimal methods [1,6,13], etc. However, to determine the learning gains involved in the PID-type ILC algorithms, relevant model information or parameter ranges of the controlled system are often required. As for the adaptive ILC algorithms, they have been mainly designed for linearly parameterized systems [17,20,21] and non-parameterized nonlinear systems [22,23]. The linearly parameterized systems are heavy model-dependent since they are modeled as a linear combination of some unknown parameters with respect to known nonlinear functions. The non-parameterized nonlinear systems based adaptive ILC algorithms normally use neural networks or fuzzy systems to approximate some unknown nonlinear dynamics such that a perfect ILC tracking performance is hardly achieved due to the approximation errors from the neural networks or fuzzy systems. Moreover, in the adaptive ILC algorithms [17,20–23], the control directions of the controlled systems are normally required to be invariable and known a priori. Notably, in many practical engineering processes, it is very difficult or expensive to obtain the exact or estimated information on mathematical model of the controlled systems. Therefore, a fully data-driven ILC approach, in which the input-output data of the controlled system is involved only, is expected.

On the other hand, the existing ILC algorithms have been mainly designed in time domain [2–5]. From an engineering point of view, a frequency-domain based ILC technique is sometimes preferable as it may exhibit the spectrum characteristics of system signals and provide the lower computation burden for convolution operation of time-domain signals. However, compared with the fruitful ILC results in time domain, the frequency-domain based ILC designs are very limited [12–15]. In [12], for linear continuous-time single-input single-output (SISO) systems, convergence conditions for the anticipatory learning control were obtained in terms of the lead-time and anticipatory learning gain. In [13], for linear discrete-time (LDT) SISO systems, a frequency-domain based ILC design was developed, which was combined with basis functions to cope with variations in tracking trajectory. In [14], three different multirate ILC algorithms using a lower sampling rate from a feedback system to update the control input were proposed for LDT SISO systems. In [15], according to the frequency spectrum features derived from the Fourier analysis to the average energy of ILC tracking error, sufficient and necessary conditions for monotonic convergence of the ILC tracking error were demonstrated for linear continuous-time systems. It is worth noting that just like the ILC designs in time domain, the relevant model knowledge of the controlled systems plays an important role in applying the frequency-domain based ILC laws [12–15].

This article aims to present completely data-driven ILC algorithms for LDT SISO systems in frequency domain. Recently, a novel adaptive Fourier decomposition (AFD) technique was utilized to identify the unknown transfer function of LDT SISO system [16]. AFD-type

techniques outperform other system identification techniques with a fast convergence rate of series for approximation and a direct representation to poles of the transfer function [33] since the basis functions of AFD are selected adaptively. In this article, according to [16], the input-output data of the LDT SISO system at the first repetition/cycle is utilized to constitute an AFD approximator. Then, two data-driven ILC algorithms with determining the learning gains from the AFD approximator are presented, in which the input-output data of LDT SISO system is merely dependent, and no model knowledge except for the linear minimum phase characteristic of the controlled system is required. As a result, the strictly monotonic convergence of the ILC tracking error is guaranteed in a deterministic way, which has not been realized by most time-domain based PID-type ILC algorithms [5,10] and adaptive ILC algorithms [17,23]. In this regard, it is noted that two AFD based ILC laws with data-driven determining techniques for learning gains were ever presented in [24]. However, the used AFD approximation method in [24] was combined with support vector machine such that the convergence of ILC tracking error was derived in statistical learning sense, and then, the convergent probability of ILC tracking error is dependent on the AFD approximating error to transfer function. The key features and contributions of the paper are summarized as follows:

- (1) In this paper, two AFD based ILC algorithms are proposed for LDT SISO systems, in which an AFD representation is utilized to approximate the unknown transfer function. No model knowledge except for the linear minimum phase characteristic of the controlled system is required.
- (2) A prominent advantage of the two proposed AFD based ILC designs over many PID-type ILC and adaptive ILC algorithms is that the strictly monotonic convergence of ILC tracking errors can be guaranteed, which is a very strong and desirable property of ILC algorithms.
- (3) Compared to the AFD based ILC work presented in [24], the strictly monotonic convergence of ILC tracking error obtained in this paper is in a deterministic way. The AFD approximating error to transfer function only affects the selection ranges of learning gains, and doesn't affect the monotonic convergence of ILC tracking error.

The rest of the paper is organized as follows: Preliminaries and problem formulation are given in Section 2. Section 3 presents the data-driven ILC designs using AFD in frequency domain. The simulation example is illustrated in Section 4. Finally, Section 5 concludes this paper.

### Nomenclature

- $\mathbb{C}$  Complex space
- $\mathbb{R}$  Real space
- $\mathbb{D}$  Unit disc in  $\mathbb{C}$
- $H^2(\mathbb{D})$  Hardy space
- $\langle \cdot, \cdot \rangle$  Inner product of two functions in Hardy space

In this paper, the sign  $|\cdot|$  represents the module of a complex number, and the used norm of the complex function  $f(e^{j\eta})$  is defined as  $\|f(e^{j\eta})\| = \sqrt{\frac{1}{2\pi} \int_0^{2\pi} |f(e^{j\eta})|^2 d\eta}$  as in [25].

## 2. Preliminaries and problem formulation

### 2.1. Mathematical foundation of AFD

Let the set of functions  $\{B_m(z^{-1})\}$  be defined by

$$B_m(z^{-1}) = \begin{cases} e_{\{a_m\}}(z^{-1}) \prod_{j=1}^{m-1} \frac{z^{-1}-a_j}{1-\bar{a}_j z^{-1}}, & m = 2, 3, 4, \dots \\ e_{\{a_1\}}(z^{-1}), & m = 1 \end{cases} \tag{1}$$

where  $z \in \mathbb{D}$ ,  $a_j \in \mathbb{D}$ , and  $e_{\{a_j\}}(z^{-1}) = \frac{\sqrt{1-|a_j|^2}}{1-\bar{a}_j z^{-1}}$ , ( $j = 1, 2, \dots, m$ ). According to the AFD theory [18], for any sequence  $\{a_j\}$  in  $\mathbb{D}$ ,  $\{B_m(z^{-1})\}$  constitutes a set of orthogonal basis functions for AFD. Specifically, if all  $\{a_j\}$  are taken to be 0,  $\{B_m(z^{-1})\}$  yields a set of Fourier basis functions [19].

For any  $F(z^{-1}) \in H^2(\mathbb{D})$ , it can be represented by the following AFD form [18]:

$$F(z^{-1}) = \sum_{m=1}^{+\infty} c_m B_m(z^{-1}) = \sum_{m=1}^M c_m B_m(z^{-1}) + R_F(z^{-1}, M) \tag{2}$$

where  $c_m = \langle F_m(z^{-1}), e_{\{a_m\}}(z^{-1}) \rangle \in \mathbb{C}$  and  $F_m(z^{-1}) = \frac{F_{m-1}(z^{-1}) - \langle F_{m-1}(z^{-1}), e_{\{a_{m-1}\}}(z^{-1}) \rangle e_{\{a_{m-1}\}}(z^{-1})}{\frac{z^{-1}-a_{m-1}}{1-\bar{a}_{m-1}z^{-1}}}$  with

$F_1(z^{-1}) = F(z^{-1})$  and  $a_m = \arg \max_{a \in \mathbb{D}} \{ |\langle F_m(z^{-1}), e_{\{a\}}(z^{-1}) \rangle|^2 \}$ , ( $m = 1, 2, \dots, M$ ).  $R_F(z^{-1}, M) = F_{M+1}(z^{-1}) \cdot \prod_{m=1}^M \frac{z^{-1}-a_m}{1-\bar{a}_m z^{-1}}$  denotes the standard remainder for AFD with the  $M$ th partial sum.

Regarding the AFD representation Eq. (2) with the standard remainder  $R_F(z^{-1}, M)$ , we have the following Lemma 1.

**Lemma 1.** [26]. Let  $F(z^{-1}) \in H^2(\mathbb{D})$  be represented as AFD in Eq. (2). Then, there is

$$\|R_F(z^{-1}, M)\| \leq \frac{L_g}{\sqrt{M}} \tag{3}$$

where  $\sum_{m=1}^{+\infty} |c_m| \leq L_g$  with  $0 < L_g < +\infty$ .

It is noted that the calculation of  $\|R_F(z^{-1}, M)\|$  is somewhat complicated. To facilitate the sequent applications of the bound on the standard remainder  $R_F(z^{-1}, M)$  in ILC designs, it is proved in Appendix that  $\|R_F(z^{-1}, M)\| \leq \frac{L_g}{\sqrt{M}}$  is equivalent to

$$|R_F(z^{-1}, M)| \leq \frac{L_g}{\sqrt{M}} \tag{4}$$

According to Lemma 1, the larger  $M$  leads to the smaller standard remainder  $R_F(z^{-1}, M)$ . Specifically,  $\lim_{M \rightarrow +\infty} R_F(z^{-1}, M) = 0$ .

### 2.2. ILC and AFD based approach

Consider the ILC issue of the following LDT SISO system performing repetitive operation over the discrete-time instants  $\{0, 1, 2, \dots, N\}$ ,

$$\begin{cases} x_k(n+1) = Ax_k(n) + Bu_k(n), \\ y_k(n) = Cx_k(n) + Du_k(n), \end{cases} \tag{5}$$

where the subscript  $k = 0, 1, 2, \dots$  indicates the iteration/repetition index, and  $n \in \{0, 1, 2, \dots, N\}$  is the discrete-time instant.  $x_k(n) \in \mathbb{R}^n$ ,  $u_k(n) \in \mathbb{R}^1$ , and  $y_k(n) \in \mathbb{R}^1$  denote the system state, input, and output, respectively.  $A, B, C$ , and  $D$  (normally,  $D = 0$ ) are system matrices with appropriate dimensions. The reference trajectory of the LDT SISO system (5) is  $y_d(n)$ ,  $n \in \{0, 1, 2, \dots, N\}$ . Then the ILC tracking error at the  $k$ -th iteration is defined as

$$e_k(n) = y_d(n) - y_k(n) \tag{6}$$

The initial iterative output of the LDT SISO system (5) is supposed to satisfy  $y_k(0) = y_d(0) = 0$  for  $k = 0, 1, 2, \dots$ . Then the LDT SISO system (5) can be transferred to the following form in frequency domain.

$$Y_k(z^{-1}) = G(z^{-1}) \cdot U_k(z^{-1}) \tag{7}$$

where  $U_k(z^{-1})$  and  $Y_k(z^{-1})$  represent the Z-transformation to  $u_k(n)$  and  $y_k(n)$ , respectively, i.e.,  $U_k(z^{-1}) = Z[u_k(n)]$  and  $Y_k(z^{-1}) = Z[y_k(n)]$ .  $G(z^{-1}) = C(z^{-1}I - A)^{-1}B + D$  is the transfer function of the LDT SISO system (5).

The goal of ILC design is to update  $U_k(z^{-1})$  or  $u_k(n)$  iteratively such that  $\lim_{k \rightarrow +\infty} E_k(z^{-1}) = 0$  or  $\lim_{k \rightarrow +\infty} e_k(n) = 0$  at  $n \in \{0, 1, 2, \dots, N\}$ , where  $E_k(z^{-1}) = Z^{-1}[e_k(n)] = Y_d(z^{-1}) - Y_k(z^{-1})$  with  $Y_d(z^{-1}) = Z[y_d(n)]$ .

**Remark 1.** For the LDT SISO system (5), if a conventional PID-type ILC law is used, it is normally not difficult to estimate necessary parameter values to determine the learning gains, e.g., the input-output coupling scalar  $CB$  for a P-type ILC law in [30]. However, for this purpose, the initial state condition  $x_k(0) = 0 \in \mathbb{R}^n$  or  $x_k(0) = x_{k+1}(0)$  is usually required. In practical applications, for an unknown LDT SISO system (5), the observability and accurate positioning on the initial state  $x_k(0)$  are often not met. Therefore, it is necessary to investigate an estimated transfer function based ILC approach for the unknown LDT system (5).

For the LDT SISO system (7) in frequency domain, the transfer function  $G(z^{-1})$  is supposed to be completely unknown in this paper. As a result, an input-output data set based approximating technique in frequency domain is needed. Fortunately, a novel AFD technique to identify the unknown transfer function  $G(z^{-1})$  was ever presented in [16], which involves a two-step approximating process. To explain the AFD identifying technique, the following Lemma 2 is used,

**Lemma 2.** Let  $G(z^{-1})$ ,  $z \in \mathbb{D}$  be a transfer function of the LDT SISO system (5). As the frequency-domain based input-output data set  $Q = \{(\vartheta_r, G(e^{j\vartheta_r})), r = 0, 1, \dots, \bar{N} - 1\}$  is obtained by sampling the frequency response of the LDT SISO system (5) with impulse input signal  $\delta(n)$ , where  $\vartheta_r = \frac{2\pi r}{\bar{N}}$  and  $\bar{N}$  denotes the number of sampling points in the boundary of unit disc  $\mathbb{D}$ . If

$$\hat{G}(z^{-1}, \bar{N}) = \frac{1}{\bar{N}} \sum_{r=0}^{\bar{N}-1} \left( \frac{G(e^{j\vartheta_r})e^{j\vartheta_r}}{e^{j\vartheta_r} - z^{-1}} \right) \tag{8}$$

then,  $\lim_{\bar{N} \rightarrow +\infty} \hat{G}(z^{-1}, \bar{N}) = G(z^{-1})$ .

The transfer function  $G(z^{-1})$ ,  $z \in \mathbb{D}$  is continuous on  $|z| = 1$ , so Lemma 2 can be directly derived from the definition of Riemann integration [27]. In terms of the function  $\hat{G}(z^{-1}, \bar{N})$

in Eq. (8), according to [16], there is

$$\left| G(z^{-1}) - \hat{G}(z^{-1}, \bar{N}) \right| < \sup_{r=0,1,\dots,\bar{N}-2} \left| G\left(e^{j\frac{2\pi}{N}(r+1)}\right) - G\left(e^{j\frac{2\pi r}{N}}\right) \right| \tag{9}$$

Letting  $F(z^{-1}) = \hat{G}(z^{-1}, \bar{N})$ , and combining Eq. (4) with Eq. (9), there is

$$\begin{aligned} \left| G(z^{-1}) - \sum_{m=1}^M c_m B_m(z^{-1}) \right| &< \left| G(z^{-1}) - \hat{G}(z^{-1}, \bar{N}) \right| + \left| \hat{G}(z^{-1}, \bar{N}) - \sum_{m=1}^M c_m B_m(z^{-1}) \right| \\ &< \sigma + \frac{L_g}{\sqrt{M}} := \phi \end{aligned} \tag{10}$$

where  $\sigma = \sup_{r=0,1,\dots,\bar{N}-2} |G(e^{j\vartheta_{r+1}}) - G(e^{j\vartheta_r})|$ .

**Remark 2.** In fact, Eq. (10) represents a two-step approximation process to the unknown transfer function  $G(z^{-1})$  by AFD. Firstly,  $G(z^{-1})$  is approximated by the data set based function  $\hat{G}(z^{-1}, \bar{N})$ . Then, the known function  $\hat{G}(z^{-1}, \bar{N})$  is expanded as AFD representation  $\sum_{m=1}^M c_m B_m(z^{-1})$ . Notably, since the transfer function  $G(z^{-1})$  is completely unknown, its AFD representation cannot be gotten directly from  $G(z^{-1})$ .

**Remark 3.** The approximation error  $\phi = \sigma + \frac{L_g}{\sqrt{M}}$  in Eq. (10) includes a residual error  $\sigma$  and a standard remainder  $\frac{L_g}{\sqrt{M}}$  to  $\hat{G}(z^{-1}, \bar{N})$  by using the AFD representation  $\sum_{m=1}^M c_m B_m(z^{-1})$ . The residual error  $\sigma = \sup_{r=0,1,\dots,\bar{N}-2} |G(e^{j\vartheta_{r+1}}) - G(e^{j\vartheta_r})|$  can be easily gotten from the data set  $Q = \{(\vartheta_r, G(e^{j\vartheta_r})), r = 0, 1, \dots, \bar{N} - 1\}$  with  $\vartheta_r = \frac{2\pi r}{N}$ . The standard remainder  $\frac{L_g}{\sqrt{M}}$  can be derived by setting  $M$  as a given value and  $L_g = \inf\{L_F : \hat{G}(z^{-1}, \bar{N}) \in H_2(\mathcal{D}, L_F)\}$ [26], where  $\mathcal{D} := \{e_{\{a_m\}}(z^{-1}), a_m \in \mathbb{D}\}$  and  $H_2(\mathcal{D}, L_F) := \{\hat{G}(z^{-1}, \bar{N}) = \sum_{m=1}^{+\infty} c_m B_m(z^{-1}) | e_{\{a_m\}}(z^{-1}) \in \mathcal{D}, \sum_{m=1}^{+\infty} |c_m| < L_F\}$  with  $B_m(z^{-1})$  defined in (1). As a consequence, the value of  $\phi$  is computable for approximating the unknown transfer function  $G(z^{-1})$ .

For subsequent ILC analysis, Assumption 1 is imposed on the LDT SISO system (5) or Eq. (7), which is often used in frequency-domain based ILC designs [11,12].

**Assumption 1.** The LDT SISO system (5) or (7) is of minimum phase, and there exists a minimum phase inverse for it.

Based on the AFD approximation (10) and Assumption 1, two data-driven ILC designs with unknown transfer function are produced in the following Section.

### 3. ILC designs using AFD in frequency domain

To clearly exhibit the  $L_g$  AFD based ILC approach, a simplified design procedure of ILC in frequency domain is depicted in Fig. 1.

#### 3.1. The extended PD-type ILC design

In this section, based on the AFD approximation to the unknown transfer function  $G(z^{-1})$ , the following extended PD-type ILC law is applied to the LDT SISO system (5) at  $n \in$

$\{0, 1, 2, \dots, N - 1\}$ ,

$$u_{k+1}(n) = u_k(n) + Z^{-1} \left[ (\lambda z^{-1} + \mu - \lambda) \left( \sum_{m=1}^M c_m B_m(z^{-1}) \right)^{-1} \cdot E_{k+1}(z^{-1}) \right] \tag{11}$$

where  $z^{-1} = e^{j\omega T}$  with sampling period  $T$  to continuous-time signal,  $Z^{-1}[\cdot]$  stands for the inverse of Z-transformation,  $\sum_{m=1}^M c_m B_m(z^{-1})$  is the AFD approximation to  $G(z^{-1})$ , and  $\lambda, \mu \in \mathbb{R}$  are learning gains.

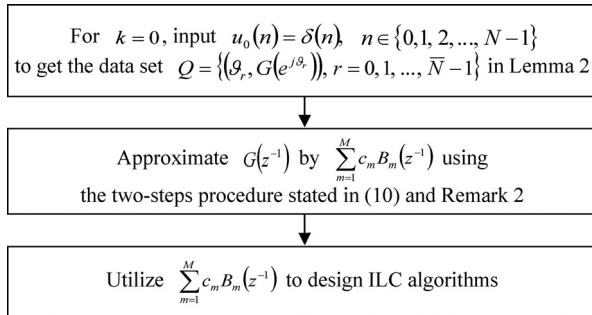


Fig. 1. AFD based ILC design procedure.

Correspondingly, the extended PD-type ILC law (11) in frequency domain is written as

$$U_{k+1}(z^{-1}) = U_k(z^{-1}) + (\lambda z^{-1} + \mu - \lambda) \left( \sum_{m=1}^M c_m B_m(z^{-1}) \right)^{-1} \cdot E_{k+1}(z^{-1}) \tag{12}$$

**Remark 4.** According to Assumption 1,  $G(z^{-1}) \neq 0, z \in \mathbb{D}$ . Therefore, from Eq. (10), we know that only if  $M$  in  $\sum_{m=1}^M c_m B_m(z^{-1})$  and the number  $\bar{N}$  of sampling points are large enough,  $\sum_{m=1}^M c_m B_m(z^{-1})$  can sufficiently approach  $G(z^{-1})$  such that  $\sum_{m=1}^M c_m B_m(z^{-1}) \neq 0$ . Subsequently, the factor  $(\sum_{m=1}^M c_m B_m(z^{-1}))^{-1}$  involved in the extended PD-type ILC law (11) or (12) is achievable.

Then, the convergence condition for the extended PD-type ILC law (11) or (12) is presented in the following Theorem 1.

**Theorem 1.** For the LDT SISO system (5) with Assumption 1, utilize the extended PD-type ILC law (11) or (12). If the learning gains  $\mu$  and  $\lambda$  in Eq. (11) or (12) make that

$$\begin{cases} \mu > \lambda > 0, \\ |\mu + 1 - 2\lambda| - \max \left\{ \left| \left( \sum_{m=1}^M c_m B_m(z^{-1}) \right)^{-1} \right| \right\} \cdot \mu \phi > 1, \end{cases} \tag{13}$$

or

$$\begin{cases} \mu + 1 < \lambda < 0, \\ |\mu + 1 - 2\lambda| + \max \left\{ \left| \left( \sum_{m=1}^M c_m B_m(z^{-1}) \right)^{-1} \right| \right\} \cdot \mu \phi > 1, \end{cases} \tag{14}$$

where  $\phi$  defined in Eq. (10) is the approximation error of  $\sum_{m=1}^M c_m B_m(z^{-1})$  to  $G(z^{-1})$ , then, the ILC tracking error  $E_k(z^{-1})$  converges strictly monotonically to zero as the iteration number  $k$  goes to infinity.

**Proof.** The ILC tracking error at the  $(k + 1)$ th trial for the LDT SISO system (5) is represented as

$$\begin{aligned} E_{k+1}(z^{-1}) &= Y_d(z^{-1}) - Y_{k+1}(z^{-1}) = E_k(z^{-1}) - (Y_{k+1}(z^{-1}) - Y_k(z^{-1})) \\ &= E_k(z^{-1}) - G(z^{-1}) \cdot (U_{k+1}(z^{-1}) - U_k(z^{-1})) \end{aligned} \tag{15}$$

Substituting (12) into (15), we have

$$E_{k+1}(z^{-1}) = E_k(z^{-1}) - G(z^{-1})(\lambda z^{-1} + \mu - \lambda) \left( \sum_{m=1}^M c_m B_m(z^{-1}) \right)^{-1} E_{k+1}(z^{-1}) \tag{16}$$

Furthermore, it yields

$$\begin{aligned} &|E_{k+1}(z^{-1})| \\ &= \frac{|E_k(z^{-1})|}{\left| 1 + G(z^{-1})(\lambda z^{-1} + \mu - \lambda) \left( \sum_{m=1}^M c_m B_m(z^{-1}) \right)^{-1} \right|} \\ &= \frac{|E_k(z^{-1})|}{\left| 1 + (\lambda z^{-1} + \mu - \lambda) + \left( G(z^{-1}) - \sum_{m=1}^M c_m B_m(z^{-1}) \right) (\lambda z^{-1} + \mu - \lambda) \left( \sum_{m=1}^M c_m B_m(z^{-1}) \right)^{-1} \right|} \\ &\leq \frac{|E_k(z^{-1})|}{\left| |\lambda z^{-1} + \mu - \lambda + 1| - \left| \left( G(z^{-1}) - \sum_{m=1}^M c_m B_m(z^{-1}) \right) (\lambda z^{-1} + \mu - \lambda) \left( \sum_{m=1}^M c_m B_m(z^{-1}) \right)^{-1} \right| \right|} \\ &\leq \frac{|E_1(z^{-1})|}{\left| |\lambda z^{-1} + \mu - \lambda + 1| - \left| \left( G(z^{-1}) - \sum_{m=1}^M c_m B_m(z^{-1}) \right) (\lambda z^{-1} + \mu - \lambda) \left( \sum_{m=1}^M c_m B_m(z^{-1}) \right)^{-1} \right| \right|^k} \end{aligned} \tag{17}$$

On the other hand, consider the following mathematical relation

$$\begin{aligned} |\lambda z^{-1} + \mu - \lambda| &= |\lambda e^{j\omega T} + \mu - \lambda| = |\lambda \cos(\omega T) + j\lambda \sin(\omega T) + \mu - \lambda| \\ &= \sqrt{(\lambda \cos(\omega T) + \mu - \lambda)^2 + \lambda^2 \sin^2(\omega T)} \\ &= \sqrt{\lambda^2 + (\mu - \lambda)^2 + 2\lambda(\mu - \lambda) \cdot \cos(\omega T)} \end{aligned}$$

where  $z^{-1} = e^{j\omega T}$ ,  $\omega \in [0, \pi/T)$ . It is noted that  $\sqrt{\lambda^2 + (\mu - \lambda)^2 + 2\lambda(\mu - \lambda) \cdot \cos(\omega T)}$  is a monotonic function on  $\omega \in [0, \pi/T)$ . As  $\omega = \pi/T$ , there is  $\sqrt{\lambda^2 + (\mu - \lambda)^2 + 2\lambda(\mu - \lambda) \cdot \cos(\omega T)} = \sqrt{\lambda^2 + (\mu - \lambda)^2 - 2\lambda(\mu - \lambda)} = |\mu - 2\lambda|$ , and as  $\omega = 0$ , there is  $\sqrt{\lambda^2 + (\mu - \lambda)^2 + 2\lambda(\mu - \lambda) \cdot \cos(\omega T)} = \sqrt{\lambda^2 + (\mu - \lambda)^2 + 2\lambda(\mu - \lambda)} = |\mu|$ . Therefore, we obtain

$$|\lambda z^{-1} + \mu - \lambda| \in [\min\{|\mu|, |\mu - 2\lambda|\}, \max\{|\mu|, |\mu - 2\lambda|\}] \tag{18}$$

$$|\lambda z^{-1} + \mu - \lambda + 1| \in [\min\{|\mu + 1|, |\mu + 1 - 2\lambda|\}, \max\{|\mu + 1|, |\mu + 1 - 2\lambda|\}] \tag{19}$$



Subsequently, there is

$$\begin{aligned}
 & \left| \lambda z^{-1} + \mu - \lambda + 1 \right| - \left| (\lambda z^{-1} + \mu - \lambda) \left( \sum_{m=1}^M c_m B_m(z^{-1}) \right)^{-1} \phi \right| \\
 & > \min \{ |\mu + 1|, |\mu + 1 - 2\lambda| \} - \phi \cdot \max \left\{ \left| \left( \sum_{m=1}^M c_m B_m(z^{-1}) \right)^{-1} \right| \right\} \cdot \max \{ |\mu|, |\mu - 2\lambda| \} \quad (20)
 \end{aligned}$$

If the learning gains  $\mu$  and  $\lambda$  in Eq. (11) or Eq. (12) make  $\mu > \lambda > 0$ , we have  $\lambda(\lambda - \mu) < 0$  and  $\left\{ |\mu + 1 - 2\lambda| - \max \{ |(\sum_{m=1}^M c_m B_m(z^{-1}))^{-1}| \} \cdot \mu \phi > 1, \lambda(\lambda - \mu - 1) < 0 \right.$  and  $\lambda(\lambda - \mu - 1) < 0$ . As a result,  $4\lambda^2 - 4\mu\lambda + \mu^2 < \mu^2$  and  $4\lambda^2 - 4\mu\lambda - 4\lambda + \mu^2 + 2\mu + 1 < \mu^2 + 2\mu + 1$ . Equivalently, there are  $|\mu - 2\lambda| < |\mu|$  and  $|\mu + 1 - 2\lambda| < |\mu + 1|$ . Thus,

$$\begin{aligned}
 & \min \{ |\mu + 1|, |\mu + 1 - 2\lambda| \} - \phi \cdot \max \left\{ \left| \left( \sum_{m=1}^M c_m B_m(z^{-1}) \right)^{-1} \right| \right\} \cdot \max \{ |\mu|, |\mu - 2\lambda| \} \\
 & = |\mu + 1 - 2\lambda| - \max \left\{ \left| \left( \sum_{m=1}^M c_m B_m(z^{-1}) \right)^{-1} \right| \right\} \cdot \mu \phi > 1 \quad (21)
 \end{aligned}$$

Similarly, if the learning gains  $\mu$  and  $\lambda$  in Eq. (11) or Eq. (12) make  $\mu + 1 < \lambda < 0$ , we obtain  $\lambda(\lambda - \mu - 1) < 0$  and  $\left\{ |\mu + 1 - 2\lambda| + \max \{ |(\sum_{m=1}^M c_m B_m(z^{-1}))^{-1}| \} \cdot \mu \phi > 1, \lambda(\lambda - \mu) < 0 \right.$  Furthermore,  $4\lambda^2 - 4\mu\lambda - 4\lambda + \mu^2 + 2\mu + 1 < \mu^2 + 2\mu + 1$  and  $4\lambda^2 - 4\mu\lambda + \mu^2 < \mu^2$ , which lead to  $|\mu + 1 - 2\lambda| < |\mu + 1|$  and  $|\mu - 2\lambda| < |\mu|$ . Consequently, the result of Eq. (21) can also be derived by the following procedure,

$$\begin{aligned}
 & \min \{ |\mu + 1|, |\mu + 1 - 2\lambda| \} - \phi \cdot \max \left\{ \left| \left( \sum_{m=1}^M c_m B_m(z^{-1}) \right)^{-1} \right| \right\} \cdot \max \{ |\mu|, |\mu - 2\lambda| \} \\
 & = |\mu + 1 - 2\lambda| - \phi \cdot \max \left\{ \left| \left( \sum_{m=1}^M c_m B_m(z^{-1}) \right)^{-1} \right| \right\} \cdot |\mu| \\
 & = |\mu + 1 - 2\lambda| + \max \left\{ \left| \left( \sum_{m=1}^M c_m B_m(z^{-1}) \right)^{-1} \right| \right\} \cdot \mu \phi \\
 & > 1.
 \end{aligned}$$

That is, whether the learning gains  $\mu$  and  $\lambda$  are selected according to Eq. (13) or Eq. (14), the result of Eq. (21) holds.

Combining Eq. (20) with Eq. (21), and considering Eq. (10), we have

$$\left| \lambda z^{-1} + \mu - \lambda + 1 \right| - \left| \left( G(z^{-1}) - \sum_{m=1}^M c_m B_m(z^{-1}) \right) (\lambda z^{-1} + \mu - \lambda) \left( \sum_{m=1}^M c_m B_m(z^{-1}) \right)^{-1} \right|$$

$$\begin{aligned}
 &> \left| \lambda z^{-1} + \mu - \lambda + 1 \right| - \left| (\lambda z^{-1} + \mu - \lambda) \left( \sum_{m=1}^M c_m B_m(z^{-1}) \right)^{-1} \phi \right| \\
 &> 1.
 \end{aligned} \tag{22}$$

At last, taking limitation on two sides of Eq. (17), and considering Eq. (22), we have

$$\lim_{k \rightarrow +\infty} E_k(z^{-1}) = 0 \tag{23}$$

Notably, it is seen from Eq. (17) that  $|E_{k+1}(z^{-1})| < |E_k(z^{-1})|$ , which means the convergence of  $E_k(z^{-1})$  is strictly monotonic. This completes the proof of Theorem 1.

**Remark 5.** In Theorem 1, the convergent condition Eq. (13) or Eq. (14) for the ILC tracking error  $E_k(z^{-1})$  reveals that the selection of learning gains  $\mu$  and  $\lambda$  is closely related to the approximating error  $\phi$  of the AFD representation  $\sum_{m=1}^M c_m B_m(z^{-1})$  to  $G(z^{-1})$ . From Eq.

(13), we have  $\begin{cases} \mu > \lambda > 0 \\ \frac{|\mu+1-2\lambda|-1}{\mu} \cdot (\max\{|\sum_{m=1}^M c_m B_m(z^{-1})\}^{-1})^{-1} > \phi \end{cases}$  and from Eq. (14), we have  $\begin{cases} \mu + 1 < \lambda < 0 \\ \frac{|\mu+1-2\lambda|-1}{-\mu} \cdot (\max\{|\sum_{m=1}^M c_m B_m(z^{-1})\}^{-1})^{-1} > \phi \end{cases}$  due to  $-\mu > 1$ . Clearly, it can be seen that the smaller the approximating error  $\phi$  is, the larger the feasible ranges of  $\mu$  and  $\lambda$  can be selected.

### 3.2. The extended P-type ILC with feedback design

In this section, the following extended P-type ILC law with feedback is applied to the LDT SISO system Eq. (5) at  $n \in \{0, 1, 2, \dots, N - 1\}$

$$u_{k+1}(n) = u_k(n) + Z^{-1} \left[ \left( \sum_{m=1}^M c_m B_m(z^{-1}) \right)^{-1} (\alpha E_k(z^{-1}) + \beta E_{k+1}(z^{-1})) \right] \tag{24}$$

where  $z^{-1} = e^{j\omega T}$ ,  $Z^{-1}[\cdot]$  stands for the inverse of Z-transformation,  $\sum_{m=1}^M c_m B_m(z^{-1})$  is the AFD approximation to  $G(z^{-1})$ , and  $\alpha, \beta \in \mathbb{R}$  stand for the learning gains. Accordingly, the extended P-type ILC law Eq. (24) in frequency domain is given by

$$U_{k+1}(z^{-1}) = U_k(z^{-1}) + \left( \sum_{m=1}^M c_m B_m(z^{-1}) \right)^{-1} (\alpha E_k(z^{-1}) + \beta E_{k+1}(z^{-1})) \tag{25}$$

Then, the convergence of the extended P-type ILC law (24) or Eq. (25) is guaranteed by the following Theorem 2.

**Theorem 2.** For the LDT SISO system (7) with Assumption 1, utilize the extended P-type ILC law (24) or Eq. (25). If the learning gains  $\alpha$  and  $\beta$  in (24) or Eq. (25) make that

$$\begin{cases} 0 < \frac{\alpha}{\beta} < 1, \\ |1 + \beta| - |\beta|\phi \cdot \max \left\{ \left| \left( \sum_{m=1}^M c_m B_m(z^{-1}) \right)^{-1} \right| \right\} > \frac{\beta + \alpha}{\beta - \alpha}, \end{cases} \tag{26}$$

where  $\phi$  defined in Eq. (10) is the approximation error of  $\sum_{m=1}^M c_m B_m(z^{-1})$  to  $G(z^{-1})$ , then, the ILC tracking error  $E_k(z^{-1})$  converges strictly monotonically to zero as the iteration number  $k$  goes to infinity.

**Proof.** Substituting the extended P-type ILC law (25) into Eq. (15), we have

$$E_{k+1}(z^{-1}) = E_k(z^{-1}) - G(z^{-1}) \left( \sum_{m=1}^M c_m B_m(z^{-1}) \right)^{-1} (\alpha E_k(z^{-1}) + \beta E_{k+1}(z^{-1})).$$

Subsequently, there is

$$\begin{aligned} |E_{k+1}(z^{-1})| &= \left| \frac{1 - \alpha \cdot G(z^{-1}) \left( \sum_{m=1}^M c_m B_m(z^{-1}) \right)^{-1}}{1 + \beta \cdot G(z^{-1}) \left( \sum_{m=1}^M c_m B_m(z^{-1}) \right)^{-1}} \right| \cdot |E_k(z^{-1})| \\ &= \left| \frac{1 - \alpha \cdot G(z^{-1}) \left( \sum_{m=1}^M c_m B_m(z^{-1}) \right)^{-1}}{1 + \beta \cdot G(z^{-1}) \left( \sum_{m=1}^M c_m B_m(z^{-1}) \right)^{-1}} \right|^k \cdot |E_1(z^{-1})| \end{aligned} \tag{27}$$

If the learning gains  $\alpha$  and  $\beta$  satisfy (26), there are  $0 < |\frac{\alpha}{\beta}| < 1$  and  $|1 + \beta| - |\beta|\phi \cdot \max\{ |(\sum_{m=1}^M c_m B_m(z^{-1}))^{-1}| \} > \frac{\beta + \alpha}{\beta - \alpha} = \frac{|1 + \frac{\alpha}{\beta}|}{1 - |\frac{\alpha}{\beta}|} > 0$ . As a result,

$$\left| \frac{\alpha}{\beta} \right| + \frac{|1 + \frac{\alpha}{\beta}|}{\left| |1 + \beta| - |\beta|\phi \cdot \max\left\{ \left| \left( \sum_{m=1}^M c_m B_m(z^{-1}) \right)^{-1} \right| \right\} \right|} < 1 \tag{28}$$

On the other hand, we have

$$\begin{aligned} &\left| \frac{1 - \alpha \cdot G(z^{-1}) \left( \sum_{m=1}^M c_m B_m(z^{-1}) \right)^{-1}}{1 + \beta \cdot G(z^{-1}) \left( \sum_{m=1}^M c_m B_m(z^{-1}) \right)^{-1}} \right| \\ &= \left| -\frac{\alpha}{\beta} + \frac{1 + \frac{\alpha}{\beta}}{1 + \beta \cdot G(z^{-1}) \left( \sum_{m=1}^M c_m B_m(z^{-1}) \right)^{-1}} \right| \\ &\leq \left| \frac{\alpha}{\beta} \right| + \frac{|1 + \frac{\alpha}{\beta}|}{\left| 1 + \beta \cdot G(z^{-1}) \left( \sum_{m=1}^M c_m B_m(z^{-1}) \right)^{-1} \right|} \\ &= \left| \frac{\alpha}{\beta} \right| + \frac{|1 + \frac{\alpha}{\beta}|}{\left| 1 + \beta + \beta \cdot \left( G(z^{-1}) - \sum_{m=1}^M c_m B_m(z^{-1}) \right) \left( \sum_{m=1}^M c_m B_m(z^{-1}) \right)^{-1} \right|} \end{aligned}$$

$$< \left| \frac{\alpha}{\beta} \right| + \frac{\left| 1 + \frac{\alpha}{\beta} \right|}{\left| |1 + \beta| - |\beta| \cdot \left| \left( G(z^{-1}) - \sum_{m=1}^M c_m B_m(z^{-1}) \right) \left( \sum_{m=1}^M c_m B_m(z^{-1}) \right)^{-1} \right| \right|} \tag{29}$$

Noting that  $|1 + \beta| - |\beta|\phi \cdot \max\{ |(\sum_{m=1}^M c_m B_m(z^{-1}))^{-1}| \} > \frac{\beta + \alpha}{\beta - \alpha} > 0$  from Eq. (26), and  $|G(z^{-1}) - \sum_{m=1}^M c_m B_m(z^{-1})| < \phi$  in (10), we have

$$\begin{aligned}
 & |1 + \beta| - |\beta| \cdot \left| \left( G(z^{-1}) - \sum_{m=1}^M c_m B_m(z^{-1}) \right) \left( \sum_{m=1}^M c_m B_m(z^{-1}) \right)^{-1} \right| \\
 & > |1 + \beta| - |\beta|\phi \cdot \left| \left( \sum_{m=1}^M c_m B_m(z^{-1}) \right)^{-1} \right| \\
 & > |1 + \beta| - |\beta|\phi \cdot \max \left\{ \left| \left( \sum_{m=1}^M c_m B_m(z^{-1}) \right)^{-1} \right| \right\} \\
 & > 0.
 \end{aligned} \tag{30}$$

According to Eqs. (30) and (28), the following can be derived from Eq. (29),

$$\begin{aligned}
 & \left| \frac{1 - \alpha \cdot G(z^{-1}) \left( \sum_{m=1}^M c_m B_m(z^{-1}) \right)^{-1}}{1 + \beta \cdot G(z^{-1}) \left( \sum_{m=1}^M c_m B_m(z^{-1}) \right)^{-1}} \right| \\
 & < \left| \frac{\alpha}{\beta} \right| + \frac{\left| 1 + \frac{\alpha}{\beta} \right|}{\left| |1 + \beta| - |\beta|\phi \cdot \max \left\{ \left| \left( \sum_{m=1}^M c_m B_m(z^{-1}) \right)^{-1} \right| \right\} \right|} \\
 & < 1.
 \end{aligned} \tag{31}$$

At last, taking limitation on two sides of Eq. (27), and considering Eq. (31), we have

$$\lim_{k \rightarrow +\infty} E_k(z^{-1}) = 0.$$

In addition, it is seen from Eq. (27) that  $|E_{k+1}(z^{-1})| < |E_k(z^{-1})|$ . Therefore, the convergence of  $E_k(z^{-1})$  is strictly monotonic. This completes the proof of Theorem 2.

**Remark 6.** Similar to Remark 5 for Theorem 1, the relation of feasible ranges of the learning gains  $\alpha$  and  $\beta$  in the proposed ILC law (24) with the AFD approximation error  $\phi$  can be analyzed from the convergent condition (26).

From (26), it is derived that  $0 < \frac{\alpha}{\beta} < 1$   
 $\frac{|1 + \beta| - \frac{\beta + \alpha}{\beta - \alpha}}{|\beta|} \cdot (\max\{ |(\sum_{m=1}^M c_m B_m(z^{-1}))^{-1}| \})^{-1} > \phi$ .

Consequently, there is  $\beta > \alpha > 0$   
 $(1 - \frac{2\alpha}{\beta(\beta - \alpha)}) \cdot (\max\{ |(\sum_{m=1}^M c_m B_m(z^{-1}))^{-1}| \})^{-1} > \phi$  or

$\beta < \alpha < 0, \beta \leq -1$   
 $\left\{ \left(1 - \frac{2}{\alpha - \beta}\right) \cdot \left(\max\left\{ \left|\left(\sum_{m=1}^M c_m B_m(z^{-1})\right)^{-1}\right|\right\}\right)^{-1} > \phi. \right.$  Obviously, to get larger feasible ranges of  $\alpha$  and  $\beta$ , a smaller value of  $\phi$  is expected.

**Remark 7.** It is worth noting that the proposed extended PD-type and P-type ILC laws with convergence conditions are fully based on the AFD approximation to the unknown transfer function  $G(z^{-1})$ , which does not require any knowledge except for the linear minimum phase characteristic of the system model (5). The learning gains involved in the proposed ILC laws can be easily derived by solving corresponding convergent conditions (13), (14), and (26). Therefore, **Theorems 1** and **2** exploit an input-output data set based ILC technique in frequency domain to unknown LDT SISO systems, which guarantees a strictly monotonic convergence of ILC tracking errors.

#### 4. Simulation example

In this section, a simulation example is given to illustrate the effectiveness of the proposed AFD based ILC designs in frequency domain for LDT SISO systems.

**Example.** Consider the ILC issue of a four-axis, closed loop DC servo selectively compliance assembly robot arm (SCARA) robot, SEIKO TT 3000 [31], which is discretized with sampling period  $T = 0.01s$  into the following LDT SISO system,

$$G(z^{-1}) = \frac{0.04109z^{-1} + 0.03571}{z^{-2} - 1.58z^{-1} + 0.657} \tag{32}$$

The system (32) is assumed to work repetitively over a finite time duration  $\{0, 1, 2, \dots, N\}$  with  $N = 100$ . The desired output is chosen as  $y_d(n) = \sum_{l=1}^{51} a_l [1 - \cos(b_l n)]$ , where  $b_1 = 0.1\pi$ ,  $b_l = 2(l - 1)\pi$ , ( $l = 2, 3, 4, \dots, 51$ ), and  $a_l = 80e^{-b_l}$ , ( $l = 1, 2, 3, \dots, 51$ ).

Assume that the initial iterative output of the system (32) is set as  $y_k(0) = 0$ . To verify the AFD based ILC designs in frequency domain, the accuracy of ILC tracking is evaluated by the following index  $ME^{(k)}$  on the mean error in frequency domain,

$$ME^{(k)} = \frac{1}{p} \sum_{i=1}^p |Y_d(e^{j\omega_i T}) - Y_k(e^{j\omega_i T})| \tag{33}$$

where  $\omega_i$ , ( $i = 1, 2, 3, \dots, p$ ) is evenly sampled at  $[0, 2\pi/T)$  with  $p = 200$ . It is noted that according to the sampling theorem in frequency domain [28], the value of  $p$  should be selected to satisfy  $p \geq N$ . In the AFD based ILC designs, the function  $\hat{G}(z^{-1}, \bar{N})$  in (11) is firstly needed, which is computed from the frequency-domain based data set  $Q = \{(\vartheta_r, G(e^{j\vartheta_r}))\}$ ,  $r = 0, 1, \dots, \bar{N} - 1$  with  $\vartheta_r = \frac{2\pi r}{\bar{N}}$  and  $\bar{N} = 200$ . As a result,  $\sigma = \sup_{r=0,1,\dots,\bar{N}-2} |G(e^{j\frac{2\pi}{\bar{N}}(r+1)}) - G(e^{j\frac{2\pi r}{\bar{N}}})| = 0.1854$  is gotten. Then, with the parameter

setting of  $M = 8$  and  $L_g = 5.12$ , the estimated transfer function  $\sum_{m=1}^M c_m B_m(z^{-1}) = \langle F_1(z^{-1}), e_{\{a_1\}}(z^{-1}) \rangle e_{\{a_1\}}(z^{-1}) + \sum_{m=2}^8 \langle F_m(z^{-1}), e_{\{a_m\}}(z^{-1}) \rangle e_{\{a_m\}}(z^{-1}) \prod_{j=1}^{m-1} \frac{z^{-1} - a_j}{1 - \bar{a}_j z^{-1}}$  in AFD form is obtained, where the values of  $a_m$ , ( $m = 1, 2, 3, \dots, 8$ ) are given in **Table 1**. As an illustration for approximation result, the curves of  $\sum_{m=1}^M c_m B_m(e^{j\omega T})$  and  $G(e^{j\omega T})$  at  $\omega \in [0, \pi/T)$  with  $T = 0.01s$  are depicted in **Fig. 2**.

Based on the above AFD approximation to the transfer function (32), our ILC simulation consists of the following two parts:

Table 1  
The values of  $a_m$  for  $m = 1, 2, \dots, 8$ .

$a_1$	$a_2$	$a_3$	$a_4$
0.9000	0.6614+ 0.3743j	0.8810– 0.1841j	0.8097+ 0.2585j
$a_5$	$a_6$	$a_7$	$a_8$
0.8141–0.3069j	–0.0899+ 0.0046j	0.9088– 0.0468j	0.4469– 0.35377j

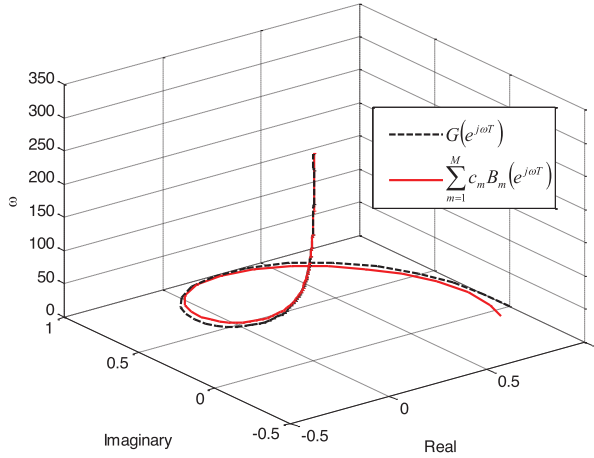


Fig. 2. Curves of  $\sum_{m=1}^M c_m B_m(e^{j\omega T})$  and  $G(e^{j\omega T})$  at  $\omega \in [0, \pi/T)$ .

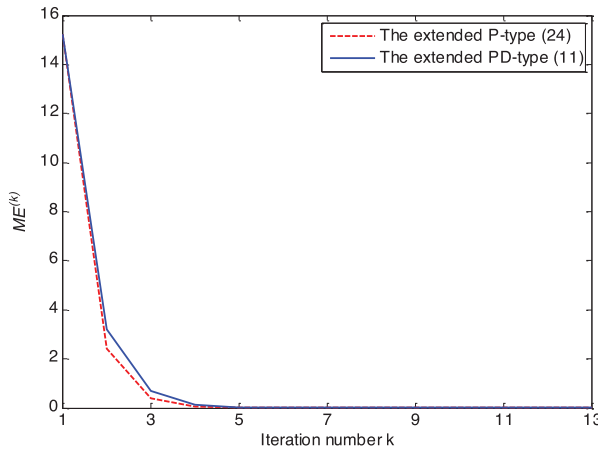


Fig. 3. ILC tracking error index  $ME^{(k)}$  at different iterations by using the two proposed AFD based ILC laws.

1) The extended PD-type ILC law (11) with the initial control input  $u_1(n) = 5.84n$  is applied to the system (32). According to Theorem 1, the values of learning gains  $\mu$  and  $\lambda$  in the ILC law (11) are chosen as  $\mu = 3.75$  and  $\lambda = 3.66$  from Eq. (14). Consequently, the solid line in Fig. 3 presents the profile of the ILC tracking error index  $ME^{(k)}$  by using the extended PD-type ILC law (11). In Fig. 4, the tracking performance of the system output

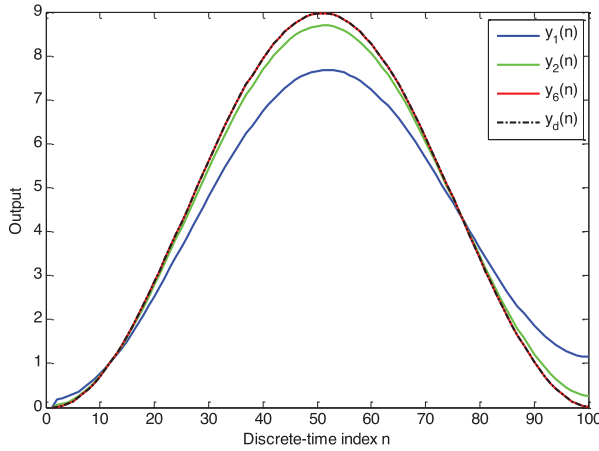


Fig. 4. Tracking performance of the system output  $y_k(n)$  to the desired trajectory  $y_d(n)$  at iterations  $k = 1$ ,  $k = 2$ , and  $k = 6$ , respectively, with the extended PD-type ILC law (11).

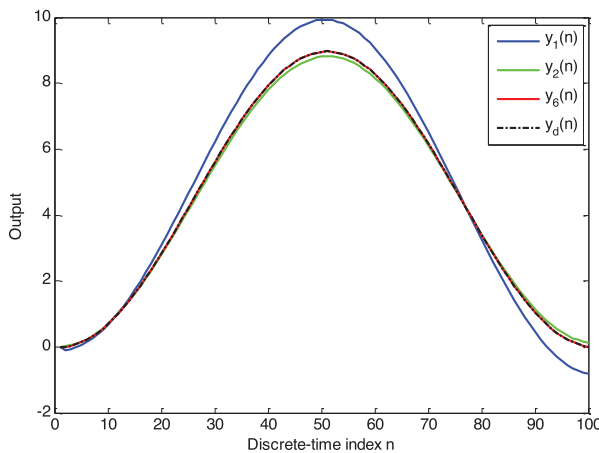


Fig. 5. Tracking performance of the system output  $y_k(n)$  to the desired trajectory  $y_d(n)$  at iterations  $k = 1$ ,  $k = 2$ , and  $k = 6$ , respectively, with the extended P-type ILC law (24).

$y_k(n)$  to the desired  $y_d(n)$  at different iterations is shown. Clearly, the extended PD-type ILC law (11) surely drives the ILC tracking error to zero strictly monotonically as the iteration number  $k$  increases. Figs. 3 and 4 are consistent with the theoretical results of the extended PD-type ILC law (11) in Theorem 1.

- 2) The extended P-type ILC law (24) with the initial control input  $u_1(n) = 5.84n$  is applied to the system (32). On the basis of Theorem 2, the values of learning gains  $\alpha$  and  $\beta$  in the ILC law (24) are taken as  $\alpha = 1.75$  and  $\beta = 3.75$  from Eq. (26). As a result, the dashed line in Fig. 3 presents the profile of the ILC tracking error index  $ME^{(k)}$  by using the extended P-type ILC law (24). And Fig. 5 shows the tracking performance of the system output  $y_k(n)$  to the desired  $y_d(n)$  at different iterations. Surely, the extended P-type ILC law (24) drives the ILC tracking error to zero strictly monotonically as the iteration number

$k$  increases. Figs. 3 and 5 verify the theoretical results of the extended P-type ILC law (24) in Theorem 2.

Regarding the comparisons of the two AFD based ILC laws (11) and (24), the computational burden of the two ILC laws is almost identical. Thanks to the efficient integration of the AFD approximation into the ILC laws, simulation results in Figs. 2–5 show no significant differences between the two AFD based ILC laws in terms of the convergence speed and the transient performance of the controlled system. Both the convergence speed of the two AFD based ILC laws are very fast.

### 5. Conclusion

To avoid the dependence of traditional ILC methods on the system model information to some extent, two completely data-driven ILC designs in frequency domain have been put forward with verification of some numerical results for the LDT SISO systems with unknown transfer functions. The designs of the proposed data-driven ILC laws are divided into two steps. During the first repetition/iteration process of ILC, the input–output data set of the LDT SISO system with a pulse signal input is used to model the unknown transfer function into an AFD representation. Then, two AFD representation based extended PD-type and P-type ILC laws with data-driven determining techniques for learning gains are presented. It has been demonstrated by mathematical proof and numerical simulation that using the two proposed data-driven ILC algorithms, the strictly monotonic convergence of ILC tracking error can be achieved in a deterministic way.

### Declaration of Competing Interest

The authors declare that they have no known competing financial interests or personal relationships that could have appeared to influence the work reported in this paper.

### Acknowledgment

This work is supported in part by the National Natural Science Foundation of China under Grant 62173354, in part by the Science and Technology Plan Project of Guangzhou under Grant 202102080656, and in part by the Science and Technology Development Fund of Macao SAR FDCT0123/2018/A3.

### Appendix. Equivalence of $\|R_F(z^{-1}, M)\| \leq \frac{L_g}{\sqrt{M}}$ to $|R_F(z^{-1}, M)| \leq \frac{L_g}{\sqrt{M}}$

**Proof.** According to the definition of norm on complex function, we have

$$\|R_F(z^{-1}, M)\| = \|R_F(e^{j\eta}, M)\| = \sqrt{\frac{1}{2\pi} \int_0^{2\pi} |R_F(e^{j\eta}, M)|^2 d\eta}, \tag{A.1}$$

where  $z^{-1} = e^{j\eta}$  with  $\eta \in [0, 2\pi)$ .

As  $|R_F(z^{-1}, M)| \leq \frac{L_g}{\sqrt{M}}$ , from Eq. (A.1), we have  $\|R_F(z^{-1}, M)\| \leq \sqrt{\frac{1}{2\pi} \int_0^{2\pi} \frac{L_g^2}{M} d\eta} = \frac{L_g}{\sqrt{M}}$ .

On the other hand, as  $\|R_F(z^{-1}, M)\| \leq \frac{L_g}{\sqrt{M}}$ , if  $|R_F(z^{-1}, M)| \leq \frac{L_g}{\sqrt{M}}$  is not true, then, there is  $|R_F(z^{-1}, M)| > \frac{L_g}{\sqrt{M}}$ . Consequently,  $\|R_F(z^{-1}, M)\| = \sqrt{\frac{1}{2\pi} \int_0^{2\pi} |R_F(e^{j\eta}, M)|^2 d\eta} >$



$\sqrt{\frac{1}{2\pi} \int_0^{2\pi} \frac{L_g^2}{M} d\eta} = \frac{L_g}{\sqrt{M}}$ . It contradicts  $\|R_F(z^{-1}, M)\| \leq \frac{L_g}{\sqrt{M}}$ . Therefore,  $\|R_F(z^{-1}, M)\| \leq \frac{L_g}{\sqrt{M}}$  is equivalent to  $|R_F(z^{-1}, M)| \leq \frac{L_g}{\sqrt{M}}$ . This completes the proof.

## References

- [1] Q. Yu, Z. Hou, J.X. Xu, X. Bu, J. Yang, Observer-based data-driven constrained norm optimal iterative learning control for unknown non-affine non-linear systems with both available and unavailable system states, *J. Frankl. Inst.* 357 (2020) 5852–5877.
- [2] J. Shi, J. Xu, J. Sun, Y. Yang, Iterative learning control for time-varying systems subject to variable pass lengths: application to robot manipulators, *IEEE Trans. Ind. Electron.* 67 (10) (2020) 8629–8637.
- [3] X. Li, Z. Zhao, F. Liu, Latent variable iterative learning model predictive control for multivariable control of batch processes, *J. Process Control* (94) (2020) 1–11.
- [4] M.K. Cobbe, K. Barton, H. Fathy, C. Vermillion, Iterative learning-based path optimization for repetitive path planning, with application to 3-D crosswind flight of airborne wind energy systems, *IEEE Trans. Control Syst. Technol.* 28 (4) (2020) 1447–1459.
- [5] K. Wan, X.D. Li, Robust iterative learning control of 2-D linear discrete FMMII systems subject to iteration-dependent uncertainties, *IEEE Trans. Syst. Man Cybern. Syst.* 99 (2019) 1–13.
- [6] S.V. Johansen, M.R. Jensen, B. Chu, J.D. Bentsen, J. Mogens, E. Rogers, Broiler FCR optimization using norm optimal terminal iterative learning control, *IEEE Trans. Control Syst. Technol.* 99 (2019) 1–13.
- [7] X.D. Li, M.M. Lv, K.L. Ho, Adaptive ILC algorithms of nonlinear continuous systems with non-parametric uncertainties for non-repetitive trajectory tracking, *Int. J. Syst. Sci.* 47 (10) (2016) 2279–2289.
- [8] J.X. Xu, A survey on iterative learning control for nonlinear systems, *Int. J. Control* 84 (7) (2011) 1275–1294.
- [9] Y. Fang, T.W.S. Chow, 2-D analysis for iterative learning controller for discrete-time systems with variable initial conditions, *IEEE Trans. Circuits Syst. I Fundam. Theory Appl.* 50 (5) (2003) 722–727.
- [10] D. Meng, K.L. Moore, Contraction mapping-based robust convergence of iterative learning control with uncertain, locally Lipschitz nonlinearity, *IEEE Trans. Syst. Man Cybern. Syst.* 50 (2) (2020) 442–454.
- [11] K.S. Hsu, Stability and analysis of iterative learning system using frequency domain method, *Int. J. Comput. Math.* 82 (11) (2006) 1339–1353.
- [12] D. Wang, Y. Ye, Design and experiments of anticipatory learning control: frequency-domain approach, *IEEE/ASME Trans. Mechatron.* 10 (3) (2005) 305–313.
- [13] F. Boeren, A. Bareja, T. Kok, T. Oomen, Frequency-domain ILC approach for repeating and varying tasks: with application to semiconductor bonding equipment, *IEEE/ASME Trans. Mechatron.* 21 (6) (2016) 2716–2727.
- [14] B. Zhang, Y. Ye, K. Zhou, D. Wang, Case studies of filtering techniques in multirate iterative learning control, *Control Eng. Pract.* 26 (3) (2014) 116–124.
- [15] X. Ruan, Z. Li, Convergence characteristics of PD-type iterative learning control in discrete frequency domain, *J. Process Control* 24 (12) (2014) 86–94.
- [16] W. Mi, T. Qian, Frequency-domain identification: an algorithm based on an adaptive rational orthogonal system, *Automatica* 48 (6) (2012) 1154–1162.
- [17] R. Chi, Z. Hou, J.X. Xu, Adaptive ILC for a class of discrete-time systems with iteration-varying trajectory and random initial condition, *Automatica* 44 (8) (2008) 2207–2213.
- [18] T. Qian, L. Zhang, Z. Li, Algorithm of adaptive Fourier decomposition, *IEEE Trans. Signal Process.* 59 (12) (2011) 5899–5906.
- [19] T. Qian, Intrinsic mono-component decomposition of functions: an advance of Fourier theory, *Math. Methods Appl. Sci.* 33 (7) (2010) 880–891.
- [20] J.X. Xu, J. Xu, On iterative learning from different tracking tasks in the presence of time-varying uncertainties, *IEEE Trans. Syst. Man Cybern. Part B Cybern.* 34 (1) (2004) 589–597.
- [21] J. Li, J. Li, Adaptive iterative learning control for consensus of multi-agent systems, *IET Control Theory Appl.* 7 (1) (2013) 136–142.
- [22] C.J. Chien, A combined adaptive law for fuzzy iterative learning control of nonlinear systems with varying control tasks, *IEEE Trans. Fuzzy Syst.* 16 (1) (2008) 40–51.
- [23] T.F. Xiao, X.D. Li, J.K.L. Ho, An adaptive discrete-time ILC strategy using fuzzy systems for iteration-varying reference trajectory tracking, *Int. J. Control Autom. Syst.* 13 (1) (2015) 222–230.
- [24] W.Y. Fu, X.D. Li, T. Qian, AFD-based ILC designs in frequency domain for linear discrete-time systems, *Int. J. Syst. Sci.* 51 (6) (2020) 3393–3407.

- [25] J.B. Garnett, *Bounded Analytic Functions*, Academic Press, 1981.
- [26] T. Qian, Y. Wang, Remarks on adaptive Fourier decomposition, *Int. J. Wavel. Multiresolut. Inf. Process.* 11 (1) (2013) 1–14.
- [27] R.G. Bartle, Return to the Riemann integral, *Am. Math. Mon.* 103 (8) (1996) 625–632.
- [28] P.P. Vaidynathan, Generalizations of the sampling theorem: seven decades after Nyquist, *IEEE Trans. Circuits Syst. I Fundam. Theory Appl.* 48 (9) (2001) 1091–1109.
- [29] X. Li, D. Shen, Two novel iterative learning control schemes for systems with randomly varying trial lengths, *Syst. Control Lett.* 107 (2017) 9–16.
- [30] J.E. Kurek, M.B. Zaremba, Iterative learning control synthesis based on 2-D system theory, *IEEE Trans. Autom. Control* 38 (2) (1993) 121–125.
- [31] B. Zhang, D. Wang, Y. Ye, Cutoff-frequency phase-in iterative learning control, *IEEE Trans. Control Syst. Technol.* 17 (3) (2009) 681–687.
- [32] C. Zeng, D. Shen, J.R. Wang, Adaptive learning tracking for robot manipulators with varying trial lengths, *J. Frankl. Inst.* 356 (2019) 5993–6014.
- [33] T. Qian, Cyclic AFD algorithm for the best rational approximation, *Math. Methods Appl. Sci.* 37 (6) (2014) 846–859.